JOURNAL OF MATERIALS SCIENCE **37** (2002) 4203–4209

Triple junction distribution profiles as assessed by electron backscatter diffraction

P. DAVIES*, V. RANDLE*, G. WATKINS†, H. DAVIES*
*Department of *Materials Engineering and †Computer Science, University of Wales, Swansea, SA2 8PP, UK*
E-mail: v.randle@swansea.ac.uk

The connectivity between the boundaries is very important because the defect character of triple junctions is expected to have a significant influence on the bulk properties of materials, particularly mechanical behaviour. The investigation of triple junction investigations presented here indicates that a restricted Coincidence Site Lattice (CSL) model was found to be the most relevant and practicable for the characterisation of triple junctions in "Grain Boundary Engineered" materials. The triple junction character distribution was measured using the automated Electron Back-Scatter Diffraction (EBSD) application of Crystal Orientation Mapping (COM) for a series of thermomechanically processed copper and alpha-brass specimens. Triple junction character statistics were determined from COM data, automatically using a custom-built computer program, utilising the CSL model. The alpha-brass data were then compared with a series of previously acquired triple junction data for a series of strain-recrystallisation copper specimens. The main aim of the investigation was to determine the relationship between the grain boundary and triple junction character distributions, which was found to be essentially a linear relationship.

1. Introduction

In recent years it has been realised that not only is the proportion of 'geometrically special' grain boundaries important to the control of properties, but also the spatial distribution and connectivity of these elements of microstructure. A straightforward approach is to study the constitution and distribution of *triple junctions*, that is, the junction line where (usually) three grains and grain boundaries meet. The defect character and other microstructural elements of triple junctions is expected to have a significant influence on the bulk properties of materials, such as mechanical behaviour [1], ductility [2], grain boundary motion [3], the susceptibility of metallic materials to intergranular degradation such as stress corrosion cracking [4–6], intergranular corrosion [7], and fracture [8]. Despite this substantial list, triple junction populations are not often measured probably because of technical difficulties in assessing accurately such distributions. In this context the objective of the present paper is two-fold: firstly to review briefly triple junction characterisation and secondly to present new data on triple junction distributions in laboratory processed copper and brass.

2. Triple junction investigations

2.1. Representation of triple junctions by the coincidence site lattice

The most popular descriptor for the geometry of grain boundaries is the coincidence site lattice (CSL) model. The CSL model can be adapted to define the geometrical characteristics of triple junctions [9, 10]. The intersection of grains resulting in a triple junction is classified according to an 'addition rule' of the Σ-value of each of the adjoining grain boundaries, where Σ refers to the reciprocal fraction of coinciding sites. For example:

$$\Sigma 9 + \Sigma 27\text{b} \rightleftharpoons \Sigma 3 \tag{1}$$

Where the general rule for a triple junction composed of Σ boundaries is that the product or quotient of two of the constituent Σ-values gives the third. A notable exception to the rule is where three $\Sigma 9$ boundaries constitute a triple junction while complying with all of the geometrical constraints. The $\Sigma 9$ boundary has a misorientation variant with an angle equal to 120° around the $\langle 511 \rangle$ axis, therefore, three boundaries of this type constitute a perfectly fitting triple junction. Grain boundaries in real polycrystals deviate from the exact Σ reference structure which means that sometimes the addition rule criterion shown for example in Equation 1 is violated. However, the misorientation of $\Sigma 3$ annealing twins is usually very close to the exact reference structure, which facilitates the efficiency of the addition rule. It has recently been proposed in the '$\Sigma 3$ regeneration model' that often the general form of the addition rule for microstructures which are dominated by $\Sigma 3^n$ boundaries is [11]:

$$\Sigma 3^n + \Sigma 3^{n+1} \rightarrow \Sigma 3 \tag{2}$$

It is convenient experimentally to characterise triple junctions by the fraction of CSL boundaries they comprise. A triple junction composed entirely of three $\Sigma 3^n$ CSL boundaries is called a 'special' triple junction because it will usually possess enhanced resistance to intergranular degradation [12]. A triple junction composed of two $\Sigma 3^n$ CSL boundaries and a single random high-angle grain boundary is also classified as 'special' because the progress of intergranular cracks and corrosion along the random high-angle grain boundary is resisted when encountering the two special grain boundaries at the triple junction [4, 12]. The remaining triple junction types are then classed as 'non-special.' A summary for the $\Sigma 3^n$ family of triple junctions is as follows:

1. Three $\Sigma 3^n$ CSL grain boundaries (special)
2. Two $\Sigma 3^n$ CSL grain boundaries (special)
3. One $\Sigma 3^n$ CSL grain boundaries (non-special)
4. Zero $\Sigma 3^n$ CSL grain boundaries (non-special)

2.2. Computer simulations

Computer simulations have been used to study the complex relationships between the grain boundary geometry distribution, the triple junction distribution and the microtexture of metallic materials [e.g., 12]. The results of one investigation determined that a randomly oriented grain/grain boundary distribution produces triple junction distributions with a U-line disclination character. The random distribution was also found to possess low proportions of CSL and CAD periodicities. An important result of the simulation was that the triple junction/line character distribution was found to be sensitive to texture (see also below). The presence of a strong fibre texture (i.e., ⟨100⟩, ⟨110⟩, ⟨111⟩) resulted in a decreasing U-line disclination content and enhanced proportions of CSL grain boundaries, triple junctions and importantly the creation of special triple junctions.

The relationship between the CSL triple junctions and CSL boundary densities [13] and CSL boundary fractions [8] has been explored by computer simulations. A further investigation [14] has provided comprehensive information on the relations between the CSL triple junction distributions and the CSL grain boundary fractions using both computer simulation and experimental studies. The results of the investigation indicate a good match between the computer simulations of fibre textures and the experimental data. The triple junction distribution was found to be highly dependent on the grain boundary geometry distribution, and specific occurrences of low-angle and twin CSL grain boundaries. A general trend was that an increase in special triple junctions resulted from an increase in proportions of CSL and CAD grain boundaries. This conclusion is logical because as the proportion of twin variant boundaries is increased in the grain boundary distribution, the probability of a twin related boundaries meeting at triple junctions should also increase.

2.3. Experimental methodologies

Triple junction distributions are most conveniently determined using Electron Back-Scatter Diffraction (EBSD) orientation mapping in a Scanning Electron Microscope (SEM). Single misorientation measurements around triple junctions can also produce triple junction character distributions but errors can occur when relying on grain identification by etching alone (see experimental work below).

There are several cases in the literature of experimental studies of triple junctions using EBSD coupled with various microstructure analyses. For example the effects of iterative strain annealing on grain boundary network of 304 stainless steel has been investigated [15], focussing specifically on the CSL boundary and the dihedral angle distributions. The thermomechanical processes improved the grain boundary character distribution, which was dominated by the $\Sigma 3$ CSL boundary but very few $\Sigma 3^n$, i.e., $\Sigma 9$ and $\Sigma 27$, boundaries were observed. The dihedral angle distribution was determined manually by measuring the angles around at least 70 triple junctions, which revealed a fairly good correlation between the CSL-based misorientation distribution and the dihedral angle distribution. An automated methodology for extracting grain boundary and surface energy from measurement of triple junction geometry has recently been developed [16] with the aim of measuring the properties of interfaces as a function of the crystallographic character. The Mesoscale Interface Mapping System (MIMS) combines computer assisted image analysis with EBSD for automatic triple-junction detection, dihedral angle geometry and crystallographic orientation measurements at each detected triple junction. The technique provides a novel approach but relies on the etching characteristics of grain boundaries on polished surfaces, which are analysed in relatively small data sets. Measurement of the grain boundary and surfaces energies of a magnesia (MgO) specimen provided a useful example of the information acquired by the technique and highlighted the importance of the dependence of grain boundary energy with inclination.

If orientation mapping is coupled with precision serial sectioning, it can successfully elucidate the 3-D structure of polycrystals and accurately determine the complete geometry of grain boundaries and triple junctions [17]. Such an analysis provides a method for extracting the relative excess free energy, and hence mobility, of grain boundaries as functions of crystallographic type from the measurement of a large number of triple junctions. However, problems with accurate registration between successive layers and the usual disadvantages of destructive techniques currently limit application.

Orientation mapping using EBSD and classification of triple junctions and boundaries by the CSL model are proving to be a popular analysis route for triple junctions, no doubt based upon practical convenience. It is this methodology, with novel local adaptations, which will be used for the present work.

3. Experimental

The objectives of the strain annealing cycles were to determine the appropriate levels of the thermomechanical variables to maximise the proportion of CSL

TABLE I Heat treatment schedules for the brass series

Spec.	Strain (%)	Time/temp (s/C)	Strain (%)	Time/temp (s/C)	Strain (%)	Time/temp (s/C)	Strain (%)	Time/temp (s/C)
SR1	25	300/665						
SR2	25	300/665	25	300/665				
SR3	25	300/665	25	300/665	10	300/665		
SR4	25	300/665	25	300/665	10	300/665	10	300/665

boundaries in the GBCD, while limiting the grain size. The thermomechanical designs for the preliminary samples were based on scaled values based on the patented treatments of Grain Boundary Engineered materials [18], in particular Alloy 600. The triple-junction character statistics are defined in this investigation by the CSL model using the Brandon ($\Sigma^{-1/2}$) criterion, which is commonly used to identify special grain boundaries. A more restrictive criterion for CSL evaluation, based on sound principles, is related to $\Sigma^{-5/6}$ [19]. The proposed Palumbo-Aust criterion $\Sigma^{-5/6}$ was shown to identify truly special grain boundaries. However, analysis of the present data indicates that since most of the $\Sigma = 3$ boundaries were very close to the exact CSL misorientation, calculation of the grain boundary character distribution by either criterion makes little difference.

A series of seven copper (Commercial Purity 99.9%) plate specimens and four alpha-brass (62/65Cu-35/38Zn) specimens had previously undergone a selection of thermomechanical treatments to attempt to alter the proportions of $\Sigma 3^n$ boundaries, i.e., to 'grain boundary engineer' them. Details of these thermomechanical treatments are given in Tables I and II [20]. Briefly, the key feature of the treatments was iterative strain-annealing cycles. Most treatments were 20–30% strain followed by a few minutes anneal at temperatures 650°C–1000°C for 1–5 cycles. The specimens were prepared for EBSD using standard metallographic techniques, ensuring that the surface grains were removed by grinding and polishing, including final polishing with colloidal silica. Sets of orientation maps

TABLE II Heat treatment schedules for the copper series

Spec.	Pre-anneal treatment	Strain (%)	Sequential heat treatments	Total number of iterations
A	1.5 h@450C	30	7 min@750 C	3
B	1.5 h@450C	67	7 min@750 C	1
C	0	0	1.5 h@450 C	1
D	1.5 h@450C	20	5 min@750 C	5
E	1.5 h@450C	30	5 min@750 C + 20 h@450 C	1
F	1.5 h@450C	20	3 min@700 C	5
G	1.5 h@450C	50	1 min@1000 C	1
H	0	0	1 h@300 C	1
J	1 H@300C	71	5 min@1000 C	1

were acquired from randomly located areas using a JEOL 6100 SEM operating at 20 kV equipped with an Oxford Instruments Opal EBSD facility. A step size of 5 μm was used for the mapping, which was appropriate to reveal annealing twins. The principles and practice of EBSD are described in detail elsewhere [21]. Fig. 1 shows an example of an orientation map set from specimen D in the copper series. Fig. 1 comprises the orientation with respect to the three orthogonal directions, a EBSD pattern quality map and a true grain map, which identifies individual grains and therefore characterises the boundaries between them by defining a 5° limit to the misorientation deviation between each pixel and excluding misorientation less than 15°. The data is then analysed and the correct triple junction character assigned to each measured junction, the triple junction distribution is the produced from a series of COMs acquired at a range of magnifications and resolutions.

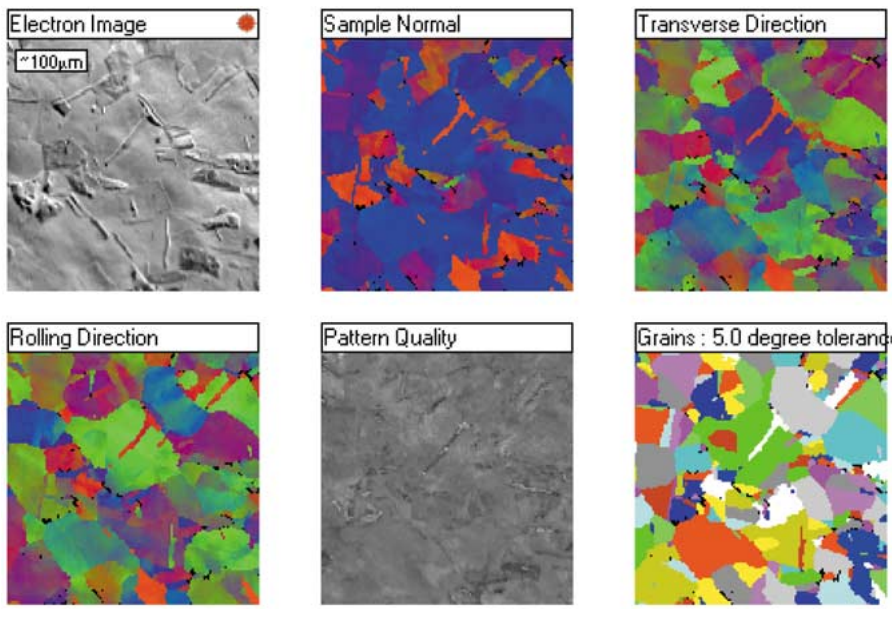

Figure 1 Examples of crystal orientation maps from the copper specimen series.

Approximately 17,000 grain boundaries were analysed in total for $\Sigma 3^n$ statistics. This figure resulted in 5225 triple junctions from the brass specimen, 1860 triple junctions from the copper specimen and an additional 600 triple junctions from manual analysis of the copper specimen (see below).

The triple junction statistics were determined automatically from orientation maps using a custom designed and built Delphi computer program, which incorporates a search algorithm that calculates and records the misorientation and classification around each triple junction present in the orientation map. This programme represents a significant advance in data analysis of triple junction populations, since it is robust and it can be performed automatically hence saving a great deal of time.

Two distinct algorithms are used to identify grain boundaries and triple junctions, the loop and stack methods. The loop method implements the basic idea of comparing every crystal grain with that of its neighbours within the matrix array. Misorientation values are calculated for each orientation measurement, starting at the top left hand corner, travelling left to right along every row until completion at the bottom right hand corner. This process is carried out using a series of loops until there is no more data to consider. The stack method is more complex than the 'loop' structure. A starting point (grain boundary) is located and the misorientations are calculated. Not only does this determine where to map a boundary at that point, but also reveals the direction that the boundary trace may be in. Since there could possibly be several directions the starting co-ordinate for each grain boundary is added to the 'stack' and is dealt with in turn, continuing the process until the 'stack' becomes empty, therefore all possible boundaries have been completed. The grain boundaries and most importantly the triple junctions are then easily characterised by both methods and then assigned the appropriate colour coded symbol, which incorporates the CSL model.

Manual EBSD analysis methods for grain junctions are reputed to entail uncertainties, particularly when identifying $\Sigma 3$ boundaries, since this class of interface is often resistant to etching. Manual analysis of grain boundaries and triple junctions involves acquiring orientation measurements across consecutive grain

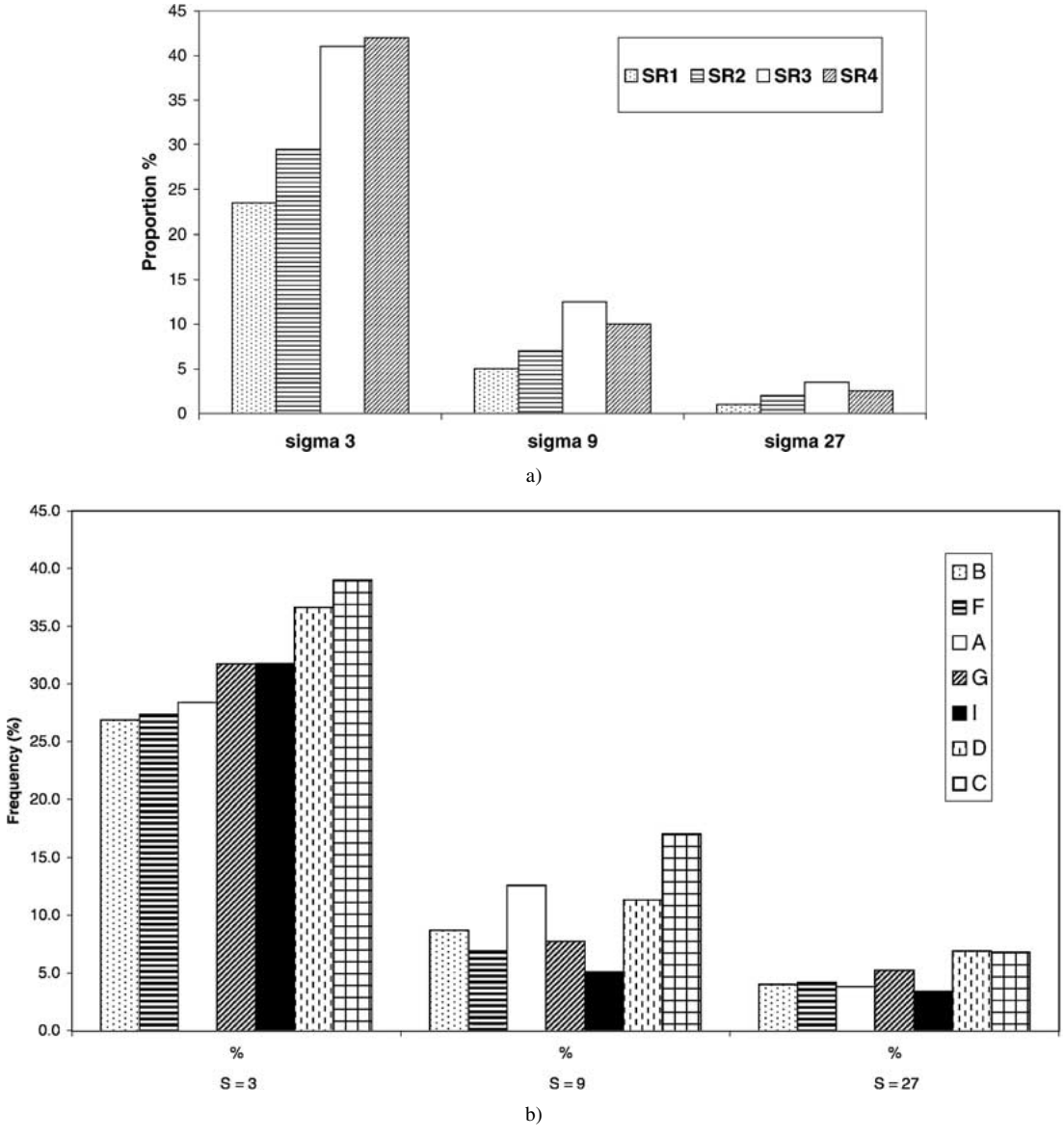

Figure 2 Proportions of $\Sigma 3^n$ boundaries after iterative strain-recrystallisation treatments in (a) brass and (b) copper.

boundaries and around each triple junction identified, by their etching characteristics, in the field of view. There is an inherent difference between grain boundary character distributions measured manually rather than acquired from a COM because of a bias related to the increased probability of encountering an annealing twin ($\Sigma = 3$), which naturally occur through grains rather than around the boundaries. However, the reliability of manual triple junction measurements is comparable with automatic detection and characterisation of triple junctions at standard resolutions ($\sim 1\ \mu m^2$). In order to test the comparative reliability of the automatic and manual method, manually acquired grain boundary and triple junction statistics were also included for the copper specimen. Finally, each measured junction was classified as 'special' or 'non-special' according to whether it comprised three/two $\Sigma 3^n$s (special) or one/zero $\Sigma 3^n$s (non-special). Proportions of $\Sigma 3^n$s ($n = 1$–3) boundaries and special triple junctions were compiled for each specimen in each of the three series (brass and copper by mapping and additionally copper by manual methods).

4. Results and discussion

Fig. 2a and b shows the breakdown of $\Sigma 3^n$ ($n = 1$–3) for the brass series and copper series respectively of iteratively heat-treated specimens, calculated from orientation maps. For every specimen in both Fig. 2a and b the majority of $\Sigma 3^n$s are $\Sigma 3$, with far fewer $\Sigma 9$s and fewer again $\Sigma 27$s. There is a difference between the brass and copper series: in the brass series of specimens the ratios of both $\Sigma 3 : \Sigma 9$ boundaries and $\Sigma 3 : \Sigma 27$ boundaries are higher than in the copper series of specimens. Fig. 3a and b shows the distribution of triple junction types for the brass series and copper series of specimens respectively. We will consider the copper series first (Fig. 3b). For every specimen except C and D the most populous triple junction group is that

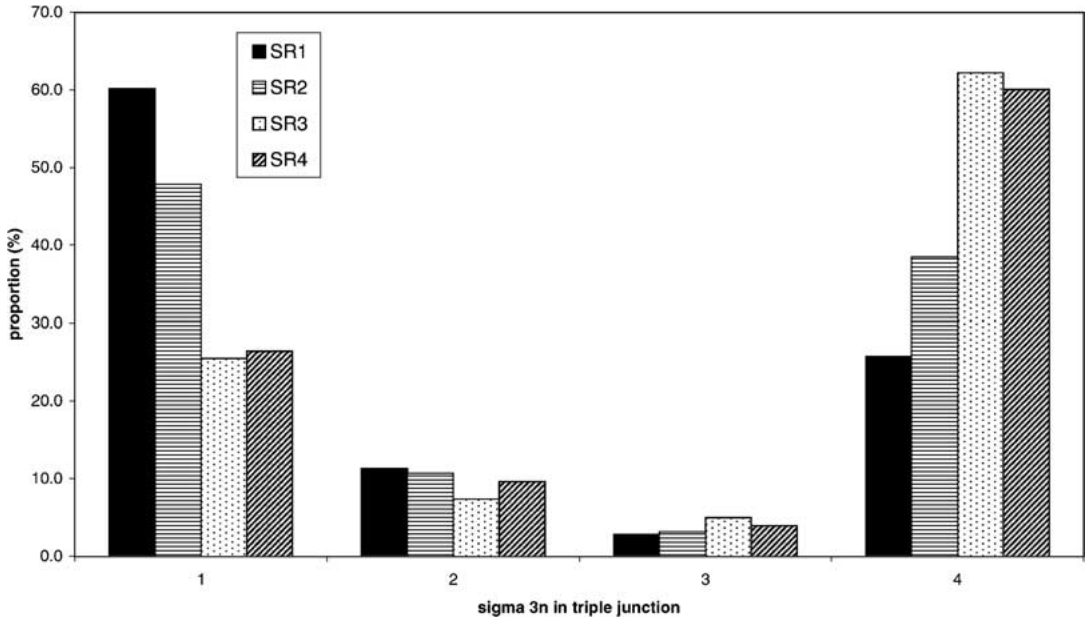

a)

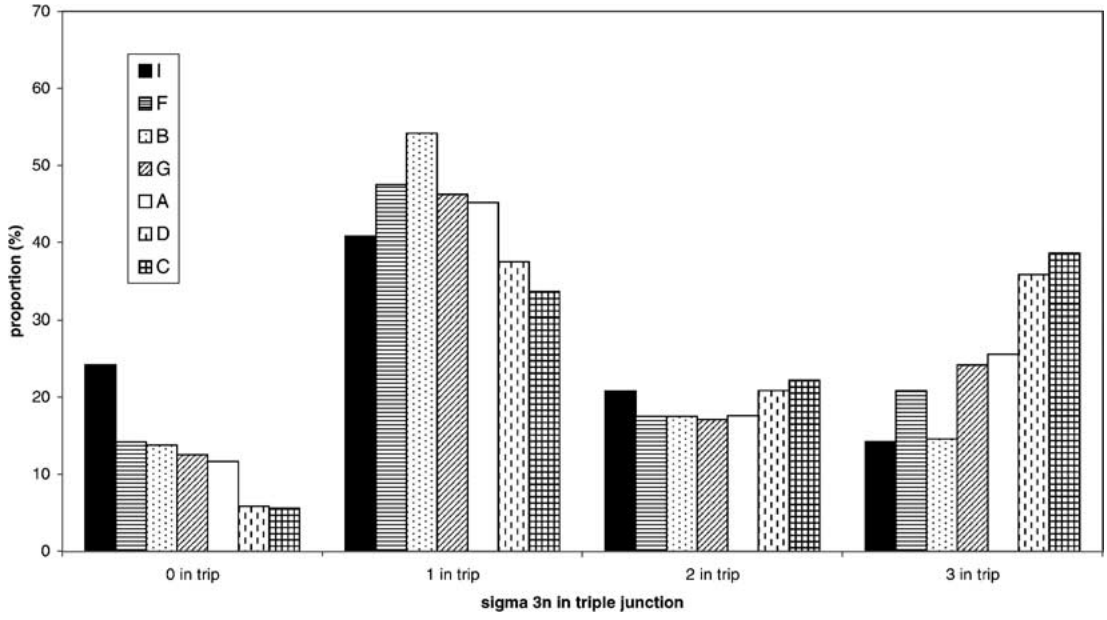

b)

Figure 3 Triple junction distribution for each specimen in (a) brass and (b) copper.

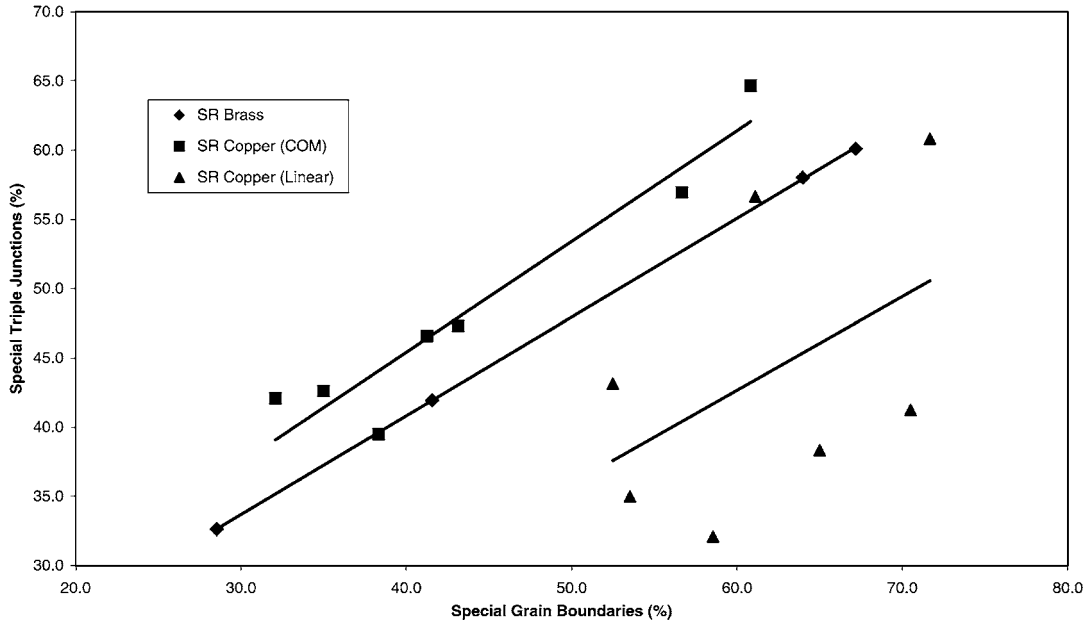

Figure 4 Relationship between proportion of $\Sigma 3^n$ boundaries and special triple junctions for the brass specimens series, the copper specimens series and the series of copper specimens where the data have been collected manually.

containing one $\Sigma 3^n$ boundary. For specimens C and D there are slightly more triple junctions having three $\Sigma 3^n$ than no $\Sigma 3^n$ triple junctions. This is consistent with the fact that specimens C and D have the highest proportion of $\Sigma 3$ boundaries, giving more chance of encounters between these boundaries to give other $\Sigma 3^n$ boundaries according to the addition rule. In an idealised microstructure if the fraction of $\Sigma 3^n$ boundaries were one-third, and if those boundaries were distributed at random, each triple junctions would contain one $\Sigma 3^n$ boundary. The data from the copper specimens contains more than one-third $\Sigma 3^n$ boundaries and, bearing in mind that many $\Sigma 9$ and $\Sigma 27$ boundaries are far from the exact Σ reference misorientation, the distribution of triple junctions in the microstructure seems to be relatively unclustered spatially.

Turning now to the brass series (Fig. 3a), in all cases only about 10% of junctions comprise one $\Sigma 3^n$, even when the proportion of $\Sigma 3^n$ boundaries is greater than one-third. The distribution is very polarised between triple junctions containing zero $\Sigma 3^n$ boundaries and those comprising three $\Sigma 3^n$ boundaries. Evidently there is considerable inhomogeneity and clustering of boundary types in the microstructure to give the distribution in Fig. 3a. The low proportions of triple junctions with two $\Sigma 3^n$ boundaries is explained by the fact that if a junction contains two boundaries which are close to the Σ reference structure, then the third is automatically also close to a Σ value. There is a jump in the proportion of special triple junctions from $<40\%$ to $>60\%$ which corresponds to the proportion of $\Sigma 3^n$ boundaries exceeding one-third. Evidently once this threshold level has been exceed the probability of interactions as is increased. For the brass series, the $\Sigma 3$-regeneration mechanism (Equation 2) has operated in the last two heat treatments (SR3 and SR4) because most triple junctions (60%) contain 3 $\Sigma 3^n$s. This conclusion is in contrast to the situation for the copper specimens, where the $\Sigma 3$-regeneration mechanism has been far less active because many triple junctions contain 1 $\Sigma 3^n$.

The distribution of special triple junctions as a function of $\Sigma 3^n$ boundaries is shown in Fig. 4 for both the brass and copper series, and also for the specimens in the copper series where the measurements have been repeated by manual methods. For the range of values reported, the proportion of special junctions increases linearly with the proportion of special boundaries, although there is far less scatter in the brass series than in the copper series (for mapped data). This is reasonable since Table I indicates that the brass specimens underwent a schedule of thermomechanical treatments comprising regular increments of strain and annealing, whereas the nature of the treatments for the copper specimens was more irregular. Furthermore, the sampling statistics were more robust for the brass specimens than for the copper specimens. The jump in proportions of special junctions and $\Sigma 3^n$ boundaries (occasioned by exceeding the threshold value for grain boundary interactions) for the (mapped) copper data is also evident in Fig. 4.

The values of $\Sigma 3^n$ proportions and special junctions for the manually collected data in the copper specimens are consistently higher than the mapping counterparts. Part of the reason for this is that manual grain boundary data are counted on a 'number' basis rather than a 'projected area' basis. But more significantly, the scatter on the manually collected data is very high, as shown in Fig. 4, which strongly suggests that the manual data are less reliable because of biased sampling and poorer statistics. The same algorithm (the stack method) is used for the calculation of triple junction statistics, regardless of if the input boundaries have been collected by manual or automatic means. The unreliability in the manual data in Fig. 4, therefore, is caused by the grain boundary data. It is striking in Fig. 4 that the gradients of the regression lines for all three series are almost parallel. The gradients for the brass and copper series (from mapping) are 0.7 and 0.8 respectively. Clearly there must be a departure from the linear relationship for low values of $\Sigma 3^n$, because when the $\Sigma 3^n$

population is zero the special junction fraction is also zero.

5. Conclusions

A novel computer programme has been generated and used to measure the proportion of triple junction types in brass and copper specimens, where the junction distribution is assessed by the proportion of $\Sigma 3^n$ types. It is shown experimentally that the different processing schedules used for the copper and brass specimens have brought about different ratios of $\Sigma 3 : \Sigma 9 : \Sigma 27$ boundaries, even though the total proportion of $\Sigma 3^n$ boundaries is similar in both the brass and the copper series. The different proportions of $\Sigma 3^n$ types resulted in markedly different triple junction profiles between the two series. The copper series is characterised by a high proportion of triple junctions having one $\Sigma 3^n$, whereas the brass series demonstrated a polarised distribution between zero and three $\Sigma 3^n$ triple junctions, indicating clustering in the microstructure. However, the rate of increase of special triple junctions (those comprising two or three $\Sigma 3^n$) to $\Sigma 3^n$ boundaries is the same for both the copper and brass series of specimens.

References

1. G. PALUMBO, U. ERB and K. T. AUST, *Scripta Metallurgica Et Materialia* **24** (1990) 2347.
2. V. B. RABUKIN, *Phys. Met .Metall.* **61** (1996) 149.
3. U. CZUBAYKO, V. G. SURSAEVA, G. GOTTSTEIN and L. S. SHVINDLERMAN, *Acta Materialia* **46** (1998) 5863.
4. K. T. AUST, U. ERB and G. PALUMBO, *Materials Science and Engineering* A **179** (1994) 329.
5. Y. PAN, B. L. ADAMS, T. OLSON and N. PANAYOTOU, *Acta Materialia* **44** (1996) 4685.
6. V. THAVEEPRUNGSRIPORN and S. W. WAS, *Metallurgical and Materials Transactions A-Physical Metallurgy and Materials Science* **28a** (1997) 2101.
7. E. M. LEHOCKEY, G. PALUMBO, P. LIN and A. M. BRENNENSTUHL, *ibid.* **29A** (1998).
8. T. WATANABE, *Materials Science and Engineering* A **174** (1994) 39.
9. E. G. DONI, G. L. BLERIS, TH. KARAKOSTAS, J. G. ANTONOPOULOS and P. DELAVIGNETTE, *Acta Crystallographica* A **41** (1985) 440.
10. W. KING, J. S. STOLKEN, M. KUMAR and A. J. SCHWARTZ, in "Electron Backscatter Diffraction in Materials Science," edited by A. J. Schwartz, M. Kumar and B. L. Adams (Kluwer, New York, 2000) p. 153.
11. V. RANDLE, *Acta Mater.* **47** (1999) 4187.
12. E. G. DONI, G. PALUMBO and K. T. AUST, *Scripta Metallurgica Et Materialia* **24** (1990) 2325.
13. K. J. KURZYDLOWSKI, B. RALPH and A. GARBACZ, *Scripta Met. Mat.* **29** (1993) 1365.
14. P. FORTIER, W. A. MILLER and K. T. AUST, *Acta Materialia* **45** (1997) 3459.
15. V. THAVEEPRUNGSRIPORN, P. SINSROK and D. THONG-ARAM, *Scripta Mat.* **44** (2001) 67.
16. B. L. ADAMS, S. TA'ASAN, D. KINDERLEHRER, I. LIVSHITS, D. E. MASON, CHUN-TE WU, W. W. MULLINS, G. S. ROHRER, A. D. ROLLETT and D. M. SAYLOR, *Interface Science* **7** (1999) 321.
17. B. L. ADAMS, D. KINDERLEHRER, W. W. MULLINS and D. ROLLET, *Scripta Met.* **38**(4) (1998) 531.
18. G. PALUMBO, International Patent no. WO 94/14986 (1994).
19. G. PALUMBO, K. T. AUST, E. M. LEHOCKEY, U. ERB and P. LIN, *Scripta Mater.* **38** (1998) 1685.
20. P. A. DAVIES, PhD Thesis University of Wales Swansea (2000).
21. V. RANDLE and O. ENGLER, "Introduction to Texture Analysis: Macrotexture, Microtexture and Orientation Mapping" (Gordon and Breach, London, 2000).

Received 11 July 2001
and accepted 14 May 2002